Int J Adv Manuf Technol (2016) 82:351–359
DOI 10.1007/s00170-015-7336-3

ORIGINAL ARTICLE

Dynamic characterization of machining robot and stability analysis

Seifeddine Mejri[1] · Vincent Gagnol[1] · Thien-Phu Le[1] · Laurent Sabourin[1] · Pascal Ray[2] · Patrick Paultre[3]

Received: 12 December 2014 / Accepted: 18 May 2015 / Published online: 11 June 2015
© Springer-Verlag London 2015

Abstract Machining robots have major advantages over cartesian machine tools because of their flexibility, their ability to reach inaccessible areas on a complex part, and their important workspace. However, their lack of rigidity and precision is still a limit for precision tasks. Innovations and design optimization of robotic structure, links, and power transmission allow robot manufacturers to propose business solutions for machining applications. Beyond accuracy problems, it is also necessary to quantify the vibration phenomena that may affect, as in machine tools, the quality of machined parts and the tools and spindle lifespan. These vibrations occurred at specific machining conditions depending on robot and spindle dynamic properties. The robot's posture evolved significantly in its workspace and induces dynamic's changes observed at the tool tip that in turn impact the stability of the machining process. The objective of this paper is to quantify the dynamic behavior's variation of an ABB IRB 6660 robot equipped with a high-speed machining (HSM) spindle in its workspace and analyze the consequences in terms of machining stability. Through an experimental modal characterization, significant variability of modal parameters is observed at the tool tip and impacts the stability of machining. The results show that an adjustment of the cutting conditions must accompany the change of robot posture during machining to ensure stability.

Keywords Modal identification · Machining robot · Chatter · Stability

✉ Seifeddine Mejri
el.mejri.seifeddine@gmail.com

[1] Institut Pascal UMR 6602 UBP/CNRS/IFMA, Clermont Université, IFMA, BP10448, 63000 Clermont Ferrand, France

[2] Ecole Nationale Supérieure des Mines de Saint Etienne, 158, cours Fauriel, 42023 Saint-Etienne Cedex 02, France

[3] Département de Génie Civil, Université de Sherbrooke, Sherbrooke, QC J1K 2R1, Canada

1 Introduction

Modern industries are heavily dependent on robots that have a wide range of applications such as material transfer, assembly, and welding. Robotic machining application for pre-machining of hard materials, or finishing operation with precise tolerances, is a segment of growth over the next years. However, many studies [1–4] have highlighted the inherent limit of articulated robots such as low repeatability and precision under large load representative of rough machining operation. Recent researches on machining robot focus on stiffness modeling [5], robot machining path planning [6], dynamics modeling, and vibration/chatter analysis including path tracking and compensation [7]. Beyond accuracy issues, it is also necessary to quantify the vibration phenomena, known as chatter vibration, that may affect, as in machine tools, the quality of machined parts and the tools and spindle lifespan. It is one of the main limitations to increase productivity as outlined by Coelho et al. [8]. These vibrations occurred at specific machining conditions, i.e., spindle speed, depth of cut and robot posture, degrade surface finish, and cause tool breakage. Tobias et al. [3] and Tlusty et al. [4] reported that two major sources are at

the origin of chatter: coupling modes and regeneration of waviness of the workpiece surface. The former one was studied by Pan et al. [2] who demonstrated that coupling modes is a cause of chatter occurrence at low frequency during robotic machining (10 Hz in their studied case). They explained it by the lack of robot's stiffness (less than 1 N/μm). However, the latter one is considered to be the most significant and important cause of machining instability in machine tool [9]. It occurs due to the modulation of the instantaneous chip thickness, cutting force variation, and subsequent tool vibration.

Although many studies have been conducted on the machining stability in milling, only few of them have considered the case of machining robots. Bisu et al. [10] have analyzed the natural frequencies of an industrial robot KUKA KR240, at three discrete positions in a restricted zone of the robot workspace. They pointed the influence of the robot's position on the natural frequencies values. However, they did not investigate the dynamic behavior at the tool tip, and consequences on milling stability did not be examined. The robot's posture evolved significantly in its workspace and induces changes in dynamic behavior at the tool tip, that in turn impact the stability of the machining process.

The objective of the paper is to study the tool tip dynamic behavior variation and investigate its consequences on the machining stability. The robot natural frequencies are identified as well as the frequency response functions (FRF) are estimated. Then, this article is organized as follows: a theoretical background of the stability lobes is presented in Section 2. Then, in Section 3, the dynamic properties of an ABB IRB 6660 robot observed at the tool tip are identified on the basis of an experimental modal analysis. The FRF analysis allows refining the frequency band of observation. Consequences on stability prediction is established and represented on stability lobes diagram. Section 4 is dedicated to the monitoring of the tool tip radial FRFs along given machining trajectory representative of the whole workspace of the ABB IRB robot. The tool tip dynamics properties variations along machining trajectories are quantified. The results obtained show significant changes in dynamic properties that affect the stability conditions. Finally, conclusion is given.

2 Milling stability background

The regenerative chatter in milling process can be illustrated by the close loop diagram presented in Fig. 1. In the current study, it will be a focus on the robot's dynamic behavior observed particularly at the tool tip.

The robot's dynamic can be represented by $H(\omega)$. The real part $R[H(\omega)]$ and the imaginary part $I[H(\omega)]$ of this function are used to determine optimal cutting parameters that maximize the chatter-free material removal rate.

$$H(j\omega) = R[H(\omega)] + jI[H(\omega)] \tag{1}$$

The milling stability method used is based on Altintas and Weck's approach [11]. In their approach, the axial force is neglected for simplicity, and two rotating force vectors acting on the tooth are considered: tangential force F_t and radial force F_r. The time-variant coefficients of the dynamic milling equations, which depend on the angular orientation of the cutter as it rotates through the cut, are expanded into a Fourier series and then truncated to include only the average component. The resulting stability relationships are shown in Eqs. 2 and 3:

$$a_{\text{lim}} = \frac{-1}{K_s.Z.R[H(\omega)]} \text{ ; with } K_s = K_t.\sqrt{1+K_r^2} \tag{2}$$

where

a_{lim} (mm): the maximum axial depth of cut.

Z : number of cutter teeth.

K_r (N/m^2): the specific cutting energy coefficient, which relates the radial cutting force F_r (N) to the tangential cutting force F_t (Fig. 2).

K_t (N/m^2) : a second specific cutting energy coefficient that relates F_t (N) to the chip area.

$$n = \frac{60}{Z.T} = \frac{2\pi.60.f_c}{Z(\pi + 2k\pi - 2\varphi)} \tag{3}$$

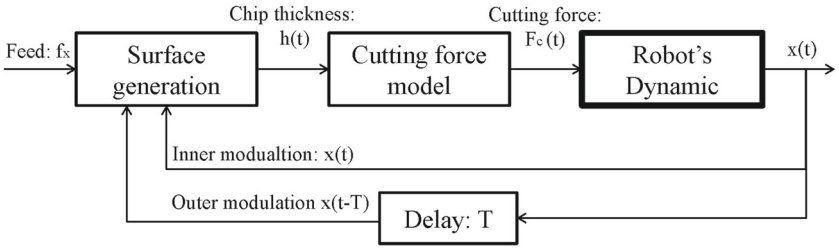

Fig. 1 Bloc diagram of regenerative chatter dynamics

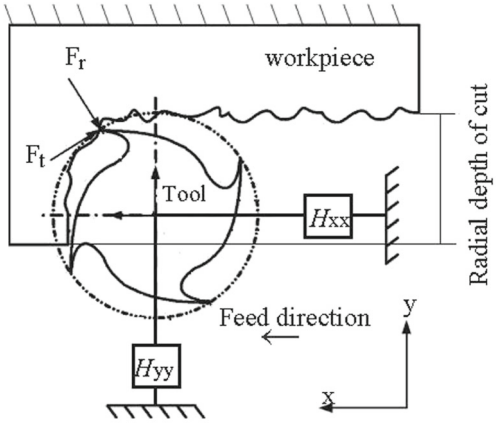

Fig. 2 The cross-sectional view of a tool tip in milling process

with $\varphi = -\tan^{-1}\left|\frac{I[H(\omega)]}{R[H(\omega)]}\right|$
n is the spindle speed (rpm), f_c is the chatter frequency (Hz), and k is an integer that corresponds to the individual lobe number. According to Eq. 2, the stability is given by the real part $R[H(\omega)]$. The depth of cut is positive only when $R[H(\omega)]$ is negative. Figure 3 shows a graphical representation of the relation between the real part and the resulting stability lobe for a milling process. The stability lobes diagram is the most common graphical illustration to represent stability information as a function of chip width and spindle speed.

This means that for the considered robotic milling process, the stability analysis requires analyzing the mode of the FRF presenting a negative real part. The robot position-dependant inertance at the tool tip node Hxx and Hyy is determined experimentally through an experimental modal analysis, respectively, in the radial direction x and y. In a second stage, a monitoring of the real part of the tool

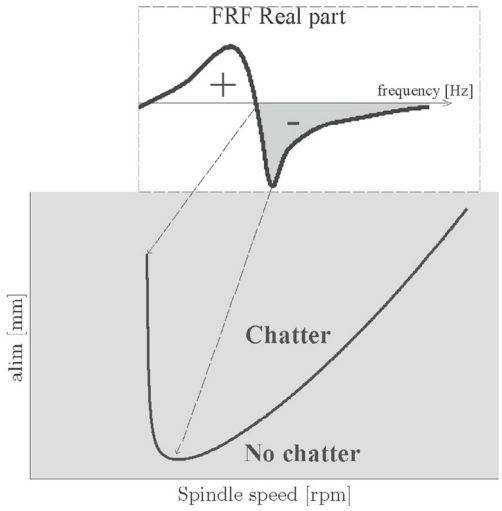

Fig. 3 Example of a FRF real part and its associated stability lobe

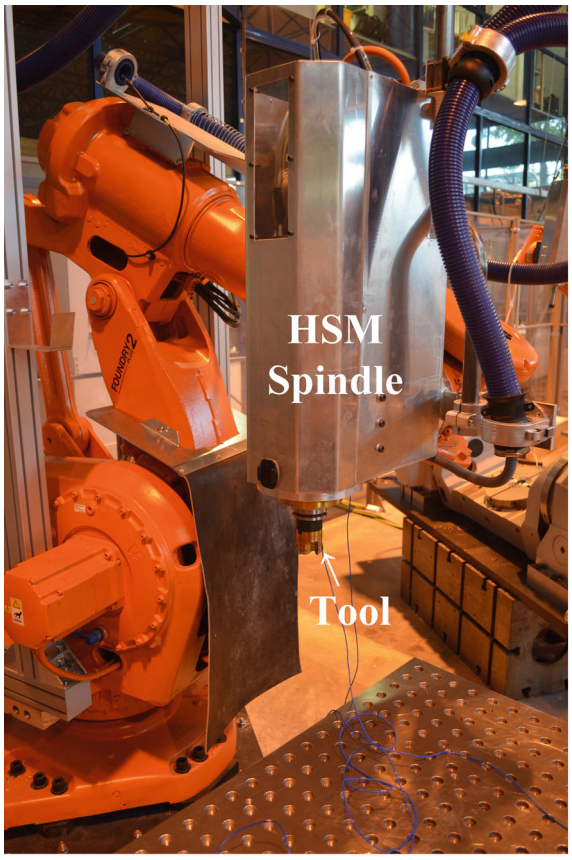

a

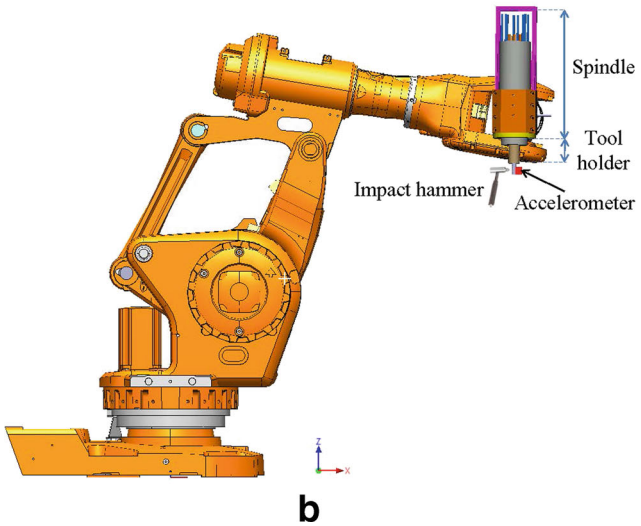

b

Fig. 4 **a** ABB IRB 6660 robot equipped with FISCHER MFW 1412/36 HSM spindle. **b** Impact and measurement on direction X

tip transfer function is required to analyze the evolution of stability along a machining trajectory.

3 Dynamic characterization and stability analysis

The machining robot is subject to different forces representative of machining forces, inertia, and control which cause static and dynamic deformation leading to tool deviation and vibration. To study the chatter phenomenon, it is important therefore to characterize the dynamic behavior of the machining robot as it is an important step of the regenerative chatter dynamics diagram as presented in Fig. 1. The result of this characterization can be represented by the robot's transfer function $H(\omega)$ and its modal parameters. The negative real part $R[H(\omega)]^-$ of the FRF is used to determine optimal cutting parameters that maximize the chatter-free material removal rate and the identified natural frequencies give information about chatter frequency originated from coupling modes.

3.1 Experimental protocol

Natural frequencies are obtained from measured FRFs. These latter are obtained by exciting the system (Fig. 4a) with an impact hammer and measuring the vibration response with accelerometers. Since the radial direction is representative of the milling excitation in a peripheral end milling operation, two tests were performed where the tool was impacted with an impact hammer (PCB Piezotronics, Model: 086D05) in two perpendicular radial directions. Only one unidirectional accelerometer (PCB Piezotronics,

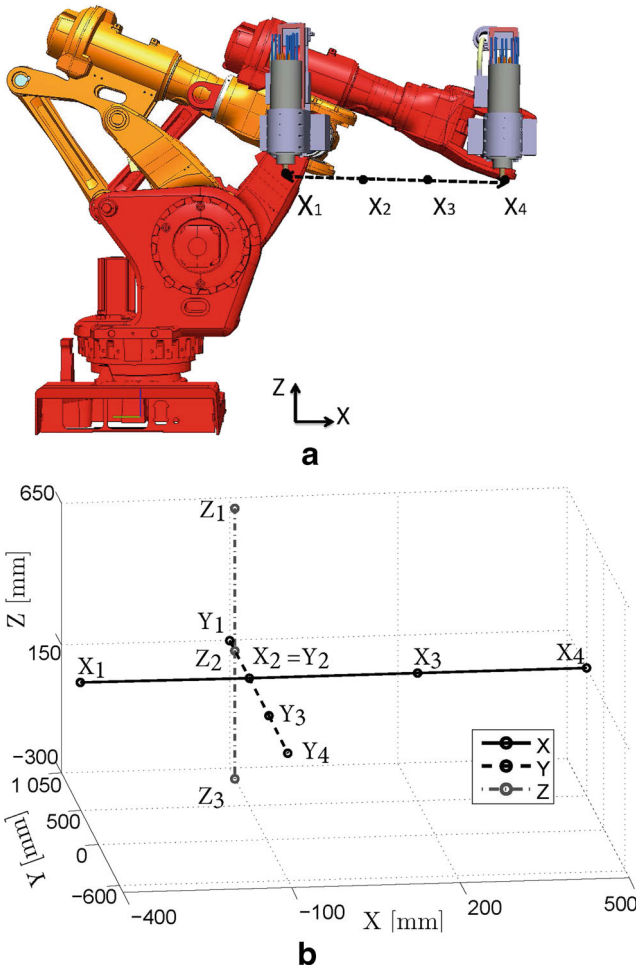

Fig. 5 **a** Robot positions along direction X. **b** Tool tip positions in the robot's workspace

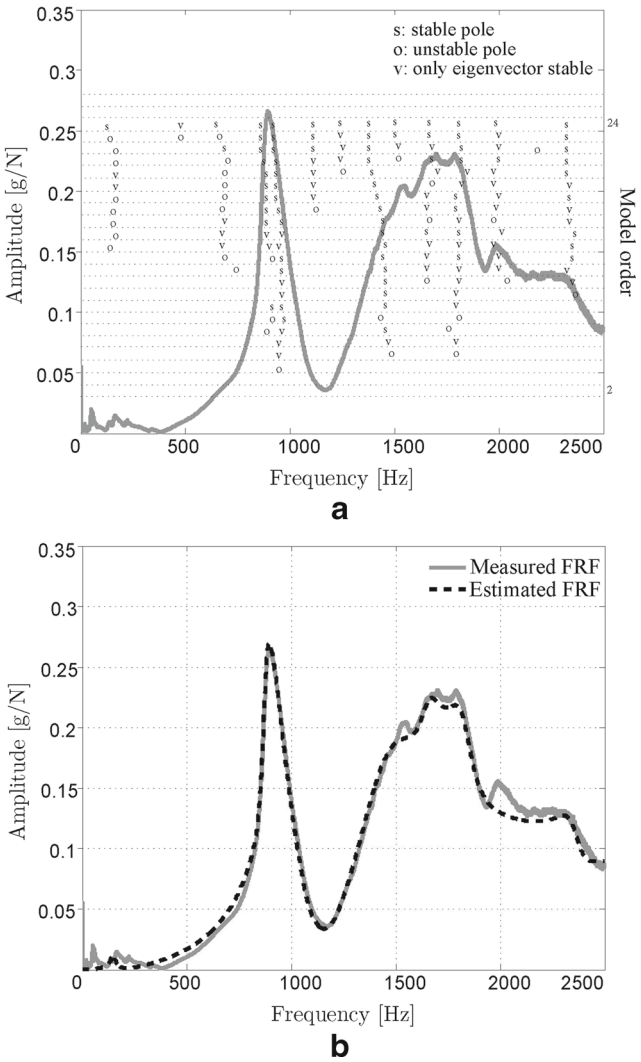

Fig. 6 Modal identification corresponding to robot position X_1 and an impact in direction X: **a** stabilization diagram, **b** measured and estimated FRF functions

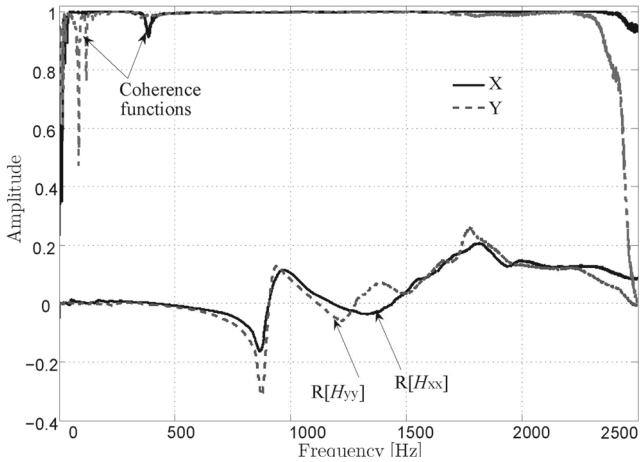

Fig. 7 Coherence and real part of the FRF functions obtained in measurement directions X and Y when robot in position X_1

Model:333C68) was fixed on the tool to avoid the effect of its mass on the measured FRF as mentioned by Özşahin et al. [12].

Figure 4b shows the impact on the tool tip in direction X and the attached accelerometer measuring vibrations in the same direction. The modal test is conducted also in the radial direction Y. The impact on the tool was repeated three times, for each measurement direction, then the average signal was analyzed. The data acquisitionwas done by a *Pimento*® system and the sampling frequency was set at 5 kHz. The frequency measurement band was (0–2500 Hz) with a frequency resolution equal to 0.305 Hz.

In order to investigate the tool tip dynamic behavior in the robot's working space, the robot was moved on the range of its limits along three specified directions X, Y, and Z (machining table referential) and a total of ten positions were investigated as shown in Fig. 5. The aim of these experiments is to observe the variation of natural frequencies values according the robot position in its workspace and consequently their influence on the stability lobe diagram.

3.2 Modal parameters identification

The natural frequencies of the tool are determined from the measured FRF curves using the *PolyMAX* method [13]. This method provides clear stabilization diagram and identifies closely spaced modes. It represents the FRFs by the so called right matrix fraction model:

$$[H(\omega)] = \sum_{r=0}^{n} z^r [\beta_r] . \left(\sum_{r=0}^{n} z^r [\alpha_r] \right)^{-1} \quad (4)$$

Where $[H(\omega)]$ contains the FRFs between i inputs and o outputs; $[\alpha_r]_{i\times i}$ and $[\beta_r]_{o\times i}$ are the denominator and

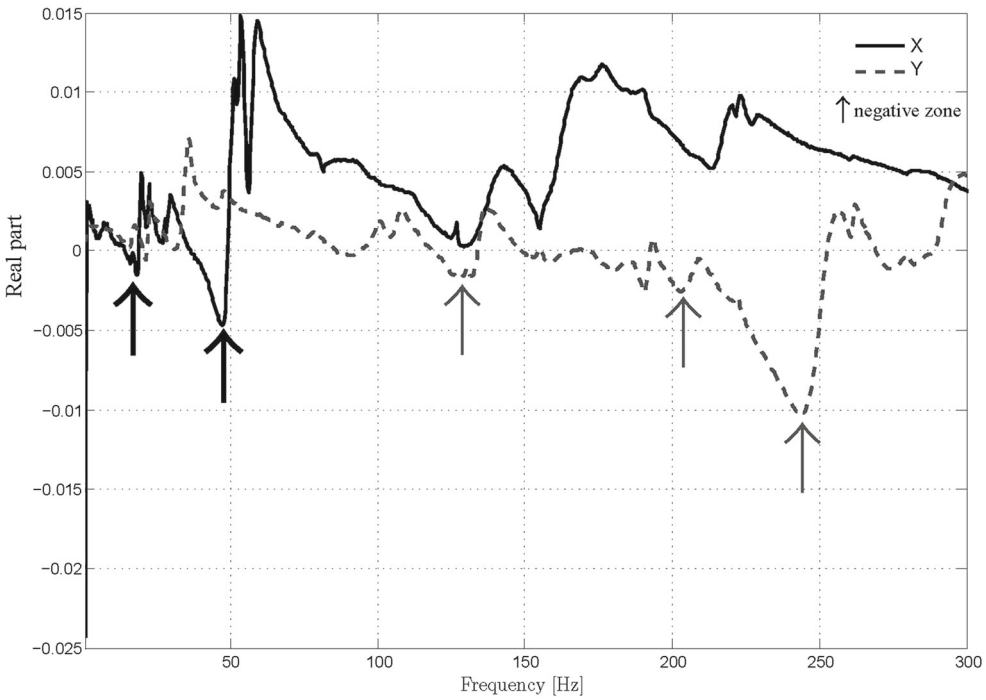

Fig. 8 Real part of the FRF in measurement directions X and Y in the frequency range (0–300 Hz)

Table 1 Identified modal parameters in the frequency range (0–300 Hz)

Mode	X		Y	
	f (Hz)	ζ (%)	f (Hz)	ζ (%)
1	19.27	4.39	34.50	4.65
2	28.78	2.73	47.75	4.18
3	50.78	5.01	108.17	3.95
4	57.07	2.82	134.33	1.76
5	137.11	6.19	207.23	1.58
6	161.57	5.17	249.97	3.90
7	217.60	1.71		

numerator matrix polynomial coefficients, respectively, n is the model order, and $z = e^{-j\omega\Delta t}$ where Δt is the sampling period. n should be selected higher than the number of expected modes in the selected frequency band. By introducing an error matrix (representative of measurement noise) between the measured FRF and the right matrix fraction model, $[\alpha_r]$ and $[\beta_r]$ are found as the least square solutions of the problem. Once the denominator coefficients are determined, poles of the model are calculated as the roots of the following equation, with $[I]$ the identity matrix:

$$\det([\alpha_0] + [\alpha_1]p + [\alpha_2]p^2 + \cdots + [I]_i\, p^n) = 0 \tag{5}$$

Since poles $p_r = e^{-\lambda_r \Delta t}$, therefore $\lambda_r = -\frac{\ln(p_r)}{\Delta t}$, usually occurring in complex conjugate pairs. The eigenfrequencies ω_r and damping ratios ξ_r are related to the complex eingenvalue λ_r as follows:

$$\lambda_r = -\xi_r\omega_r + j\omega_r\sqrt{1-\xi_r^2} \tag{6}$$

More details about the calculation procedure can be found in [14, 15].

The quality of the estimated FRF can be checked by calculating a correlation and error percentages:

$$\text{correlation} = \frac{\left|\sum_u \left(S_u \times M_u^*\right)\right|^2}{\sum_u \left(S_u \times S_u^*\right)\sum_u \left(M_u \times M_u^*\right)} \tag{7}$$

$$\text{error} = \frac{\sum_u (S_u - M_u) \times (S_u - M_u)^*}{\sum_u \left(S_u \times S_u^*\right)} \tag{8}$$

with S_u is the complex value of the synthesized FRF at spectral line u, M_u is the complex value of the measured FRF at spectral line u, and $\cdot^*$ denotes the complex conjugate.

The correlation (7) is the normalized complex product of the synthesized and measured FRFs values. And the error (8) is the least square difference normalized to the synthesized values. In the studied case, the estimated FRF presented in Fig. 6b have a correlation higher than 99 % and an error less than 1 %.

3.3 Modal identification results

The coherence function depicted in Fig. 7 indicates a good linear relationship between the impact signal and the accelerometer response and no significant noise is biasing the FRF measurements. A first observation of the real part of each of the transfer functions Hxx and Hyy shows negative values associated to modes at 880.25 and 892.71 Hz, respectively, in direction X and Y. These frequencies are influenced mainly by the modal properties of the assembly tool-tool holder-spindle. Indeed, in earlier studies [16] using the same robot and spindle but a different milling tool, a dominant natural frequency was identified at 670 Hz. Then, a zoom in the range of (0–300 Hz) is applied in order to identify the low frequency structural modes of the machining robot (Fig. 8). Among the identified frequencies (Table 1), only few of them present negative values of the real part $R[H(\omega)]$.

3.4 Stability lobes prediction

Assuming a rigid aluminium alloy AW7050 workpiece, the stability lobes were calculated using Eqs. 2 and 3 and taking

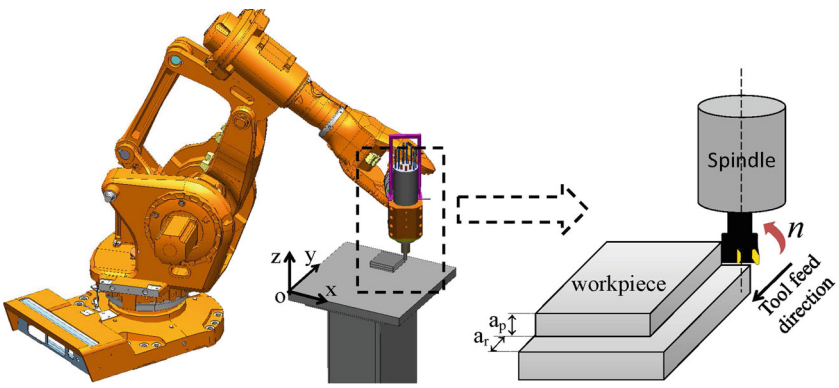

Fig. 9 Milling operation with an ABB IRB 6660 robot

a specific cutting force K_s = 660 MPa for a feed per tooth f_z = 0.1 mm. A milling tool with four teeth is considered to operate in two trajectories represented by direction X and Y (Fig. 9).

Figure 10 presents the stability lobe diagrams calculated from $R[H_{xx}(\omega)]$ and $R[H_{yy}(\omega)]$. Only regions 3^x and 4^y in the real parts of the estimated FRFs, which corresponds to the dominant mode of the assembly tool-tool holder-spindle, gave intersected stability lobes. Therefore, they will focus only on the dominant natural frequency for the robot position-dependent dynamics analysis.

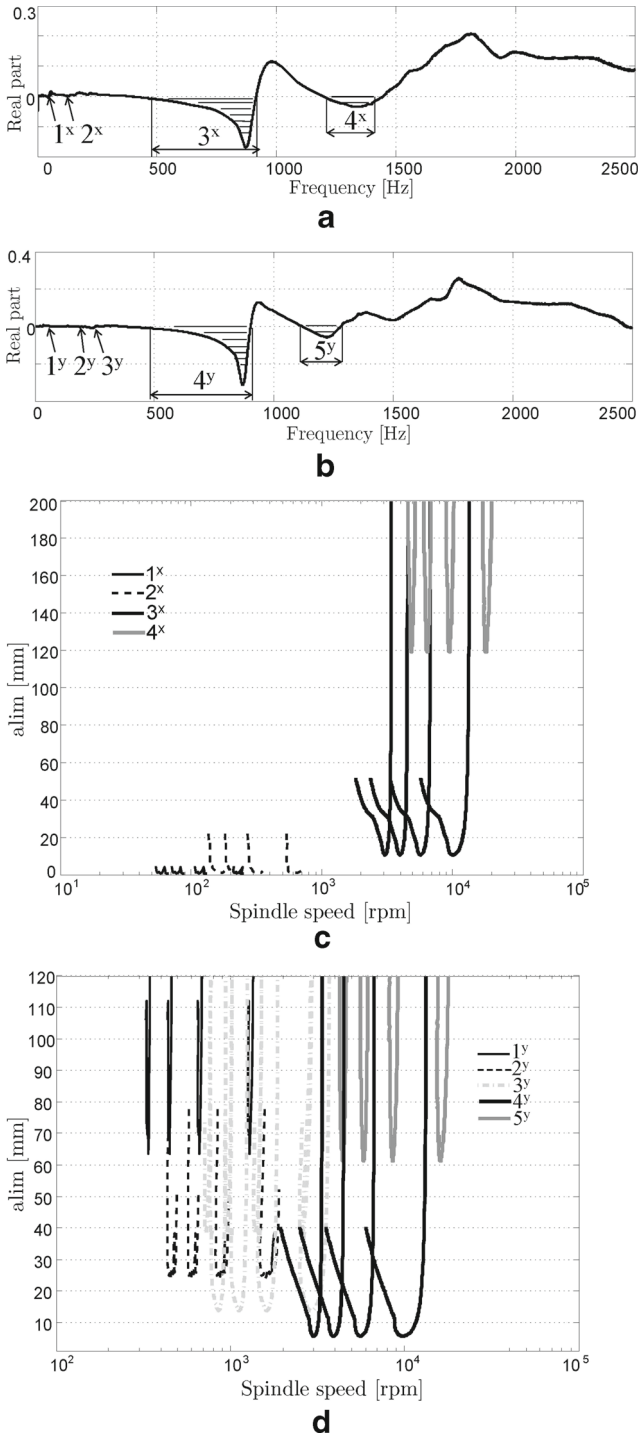

Fig. 10 **a** $R[H_{xx}]$, **b** $R[H_{yy}]$, **c** stability lobes in direction X, and **d** stability lobes in direction Y

4 Robot's position influence

The identification results in the case of an impact in direction X are given in Fig. 11. The dominant mode shows a position dependent behavior where the identified natural frequencies are estimated between 873.62 and 921.22 Hz and the damping ratios vary between 0.51 and 4.78 %. However, for the investigated positions, the machining robot dynamic behavior in radial direction Y was stable as it is indicated by the standard deviations of the identified frequencies values and damping ratios which was equal to 1.81 Hz and 0.23 %, respectively. It means that the machining robot is more rigid in radial direction Y.

Figure 11 presents the identified real parts of the dominant mode and the calculated stability lobes for the investigated robot positions with an impact in direction X. A variation of the axial depth of cut value and the spindle speed can be observed for different robot positions. The axial depth of cut have a maximum deviation equal to 3.98, 4.54, and 0.98 mm in case of robot position variation along X, Y, and Z axes, respectively. This deviation is mainly due to the dynamic stiffness variation of the dominant mode, which is dependent on the static stiffness. However, the position change did not affect the result of the stability lobes calculated from the FRF Hyy. Indeed, the dynamic variation is due to the robot configuration, where the impact in direction X modifies particularly the rotational wrist's compliance around its axis, contrary to an impact in direction Y, where the robot configuration appears stiffer.

Based on the calculated stability lobes diagrams, two ways of milling operation have to be considered. The first way, the suggested one, is to machine a workpiece while having the major cutting force component's direction parallel to the robot wrist axis. The machining robot dynamics is not position-dependent during this operation. The second way is when the major cutting force component direction is perpendicular to the robot wrist axis. In this case, the cutting parameters must be selected with respect to the robot position.

A practical method employed to avoid chatter occurrence, in machine tools, is to control the spindle speed online [17]. In another perspective, as the machining stability is associated to the closed loop stiffness between machining system dynamics and the process dynamics [18], the dynamic stiffness of the machining robot may be addressed by an adaptive control and a smart control of the kinematic

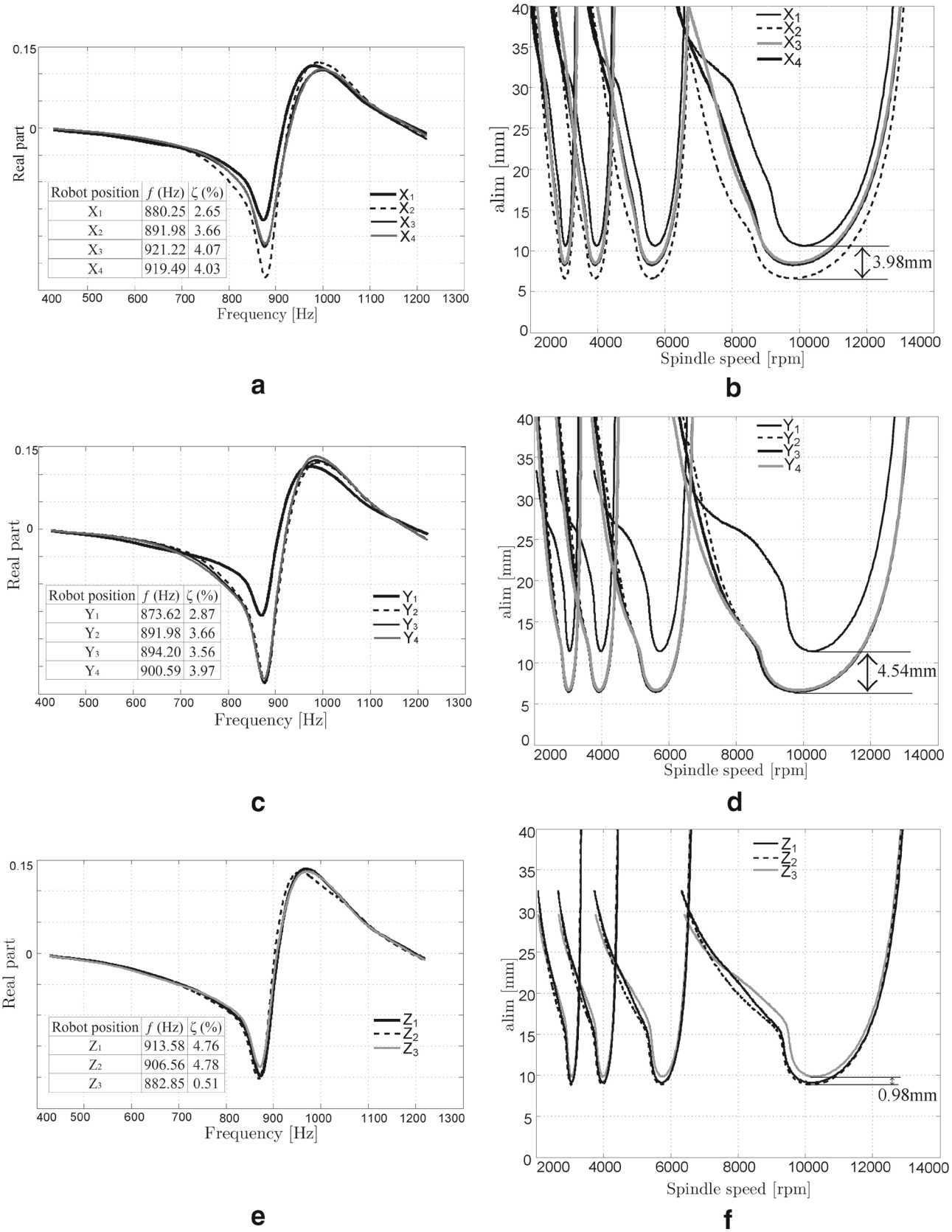

Fig. 11 Displacement along X direction: **a** R[H_{xx}], **b** stability lobes. Displacement along Y direction: **c** R[H_{xx}], **d** stability lobes. Displacement along Z direction: **e** R[H_{xx}], **f** stability lobes

redundancy, which presents the advantage of using machining robot, known for their potential to a better control handling than machine tools.

5 Conclusion

An experimental modal analysis of a milling tool mounted on a machining robot has been performed and presented in this paper. The aim of the modal tests was to calculate the stability lobes using Altintas and Weck's approach. An identification of the machining robot modal parameters was first established using PolyMAX method. Then, the stability lobes were established based on the estimated FRF, particularly on the negative real part frequency range around the dominant mode. The experimental results for the robot dynamic characterization show that they are influenced by the robot's position and the excitation direction. Therefore, the stability lobes elaborated on the identified FRF showed also robot position-dependent behavior particularly in the direction perpendicular to robot wrist axis. The stability prediction, in the case of exciting the tool tip in the same direction as the robot wrist axis, was not influenced by the robot position. It can also be noticed that the limit axial depth of cut was lower than in the case of exciting the tool tip in the direction perpendicular to robot wrist axis. Thus, the feed direction appears as an important parameter on the machining operation's stability and has to be selected carefully with consideration to the robot configuration. Further studies will be conducted to identify the robot dynamics and the influence of robot's posture in operational conditions.

Acknowledgements This work has been sponsored by the French government research program Investissements d'avenir through the IMobS3 Laboratory of Excellence (ANR-10-LABX-16-01), by the European Union through the program Regional competitiveness and employment 2007-2013 (ERDF Auvergne region), and by the Auvergne region.

References

1. Chen Y, Dong F (2013) Robot machining: recent development and future research issues. Int J Adv Manuf Technol 66(9-12):1489–1497
2. Pan Z, Zhang H, Zhu Z, Wang J (2006) Chatter analysis of robotic machining process. J Mater Process Technol 173(3):301–309
3. Tobias SA, Fishwick W (1958) The chatter of lathe tools under orthogonal cutting conditions. ASME, Trans 80(5): 1079–1088
4. Tlusty J, Polacek M (1963) The stability of the machine tool against self-excited vibration in machining. ASME Int Res Production 1:465–474
5. Abele E, Weigold M, Rothenbücher S (2007) Modeling and identification of an industrial robot for machining applications. CIRP Ann Manuf Technol 56(1):387–390
6. Olabi A, Bearee R, Nyiri E, Gibaru O (March 2010) Enhanced trajectory planning for machining with industrial six-axis robots. In: IEEE international conference on industrial technology (ICIT), pp 500–506
7. Zhang H, Wang J, Zhang G, Gan Z, Pan Z, Cui H, Zhu Z (2005). In: Proceedings IEEE/ASME international conference on advanced intelligent mechatronics, 2005. pp 1127–1132
8. Coelho ReginaldoT, Rodella HugoHT, Martins ViníciusF, Rossana Barba J (2011) An investigation into the use of industrial robots for machining soft and low density materials with hsm technique. J Braz Soc Mech Sci Eng 33:343–350
9. Altintaş Y (2000) Manufacturing Automation: Metal Cutting Mechanics, Machine Tool Vibrations, and CNC Design. Cambridge University Press
10. Bisu C-F, Cherif M, Gérard A, K'Nevez J-Y (2012) Dynamic behavior analysis for a six axis industrial machining robot, ArXiv e-prints
11. Altintaş Y, Weck M (2004) Chatter stability of metal cutting and grinding. CIRP Ann Manuf Technol 53(2):619–642
12. Özşahin O, Özgüven HN, Budak E (2010) Analysis and compensation of mass loading effect of accelerometers on tool point frf measurements for chatter stability predictions. Int J Mach Tools Manuf 50(6):585–589
13. Peeters B, Van der Auweraer H, Guillaume P, Leuridan J (2004) The polymax frequency-domain method: a new standard for modal parameter estimation Shock Vib 11(3-4): 395–409
14. Guillaume P, Verboven P, Vanlanduit S, Van der Auweraer H, Peeters B A poly-reference implementation of the least-squares complex frequency-domain estimator. In: proceedings of IMAC XXI, the International Modal Analysis Conference, Kissimmee (FL), USA, p 2003
15. Peeters B, Guillaume P, Van der Auweraer H, Cauberghe B, Verboven P, Leuridan J Automative and aerospace applications of the polymax modal parameter estimation method. In: proceedings of IMAC XXII, the International Modal Analysis Conference, Dearborn (MI)USA, p 2004
16. Mejri S, Gagnol V, Le T-P, Sabourin L, Ray P, Paultre P (2014) Analysis of machining robot configuration variation on tool tip frf measurements. In: XIX Symposium VISHNO, Aix en Provence, France
17. Liao YS, Young YC (1996) A new on-line spindle speed regulation strategy for chatter control. Int J Mach Tools Manuf 36(5):651–660
18. Cheng K (2009) Machining Dynamics - Fundamentals, Applications and Practices. Springer, London